Environmental Science & Technology

Article

pubs.acs.org/est

Light Absorption Properties and Radiative Effects of Primary Organic Aerosol Emissions

Zifeng Lu,*[,†] David G. Streets,[†] Ekbordin Winijkul,[†] Fang Yan,[†] Yanju Chen,[‡] Tami C. Bond,[‡] Yan Feng,[§] Manvendra K. Dubey,[∥] Shang Liu,[∥] Joseph P. Pinto,[⊥] and Gregory R. Carmichael[#]

[†]Energy Systems Division, Argonne National Laboratory, 9700 South Cass Avenue, Argonne, Illinois 60439, United States

[‡]Department of Civil and Environmental Engineering, University of Illinois at Urbana−Champaign, 205 North Mathews Avenue, Urbana, Illinois 61801, United States

[§]Environmental Science Division, Argonne National Laboratory, 9700 South Cass Avenue, Argonne, Illinois 60439, United States

[∥]Earth and Environmental Sciences Division, Los Alamos National Laboratory, P.O. Box 1663, Los Alamos, New Mexico 87545, United States

[⊥]National Center for Environmental Assessment, U.S. EPA, 4930 Page Road, Research Triangle Park, Durham, North Carolina 27709, United States

[#]Department of Chemical and Biochemical Engineering, The University of Iowa, 4133 Seamans Center, Iowa City, Iowa 52242, United States

Supporting Information

ABSTRACT: Organic aerosols (OAs) in the atmosphere affect Earth's energy budget by not only scattering but also absorbing solar radiation due to the presence of the so-called "brown carbon" (BrC) component. However, the absorptivities of OAs are not represented or are poorly represented in current climate and chemical transport models. In this study, we provide a method to constrain the BrC absorptivity at the emission inventory level using recent laboratory and field observations. We review available measurements of the light-absorbing primary OA (POA), and quantify the wavelength-dependent imaginary refractive indices (k_{OA}, the fundamental optical parameter determining the particle's absorptivity) and their uncertainties for the bulk POA emitted from biomass/biofuel, lignite, propane, and oil combustion sources. In particular, we parametrize the k_{OA} of biomass/biofuel combustion sources as a function of the black carbon (BC)-to-OA ratio, indicating that the absorptive properties of POA depend strongly on burning conditions. The derived fuel-type-based k_{OA} profiles are incorporated into a global carbonaceous aerosol emission inventory, and the integrated k_{OA} values of sectoral and total POA emissions are presented. Results of a simple radiative transfer model show that the POA absorptivity warms the atmosphere significantly and leads to ∼27% reduction in the amount of the net global average POA cooling compared to results from the nonabsorbing assumption.

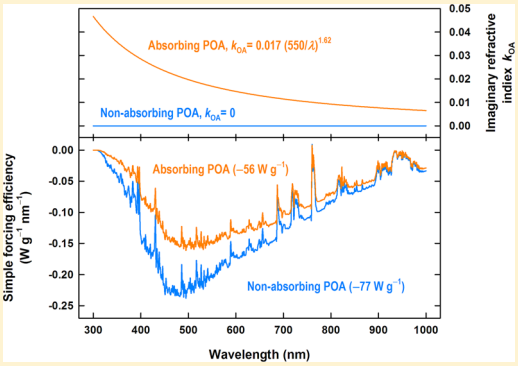

INTRODUCTION

Atmospheric carbonaceous aerosols (i.e., black carbon, BC, and organic aerosol, OA) affect Earth's energy budget by scattering and absorbing solar radiation. While BC is commonly considered to be the second most important global warming agent in the atmosphere (after only CO_2),[1] OA is typically treated as a cooling agent that purely scatters solar radiation. However, recent studies showed that OA components can also contribute substantially to light absorption. In contrast to BC, which absorbs light throughout the UV−vis spectrum, the so-called "brown carbon" (BrC) component in OA absorbs mostly in the near-UV and blue wavelength and exhibits stronger wavelength dependence.[2] BrC has been widely observed in biomass/biofuel[3−18] and fossil fuel[14,19−23] combustion sources, and the inclusion of its contribution in climate and chemical transport models has been shown to improve the simulations of aerosol light absorption significantly.[24,25] BrC has been reported to be responsible for from ∼20% to >50% of the aerosol light absorption at UV wavelengths[23−29] and thus could perturb the radiative balance and influence tropospheric photochemistry.

Knowledge of the optical properties of primary OA (POA) emissions is essential in modeling their climate effects. The complex refractive index ($m = n - ik$) is the fundamental parameter determining the particles' optical properties, where the real (n) and the imaginary (k) parts represent the scattering and absorbing components, respectively. For example, the mass

Received: January 13, 2015
Revised: March 20, 2015
Accepted: March 26, 2015
Published: March 26, 2015

DOI: 10.1021/acs.est.5b00211
Environ. Sci. Technol. 2015, 49, 4868−4877

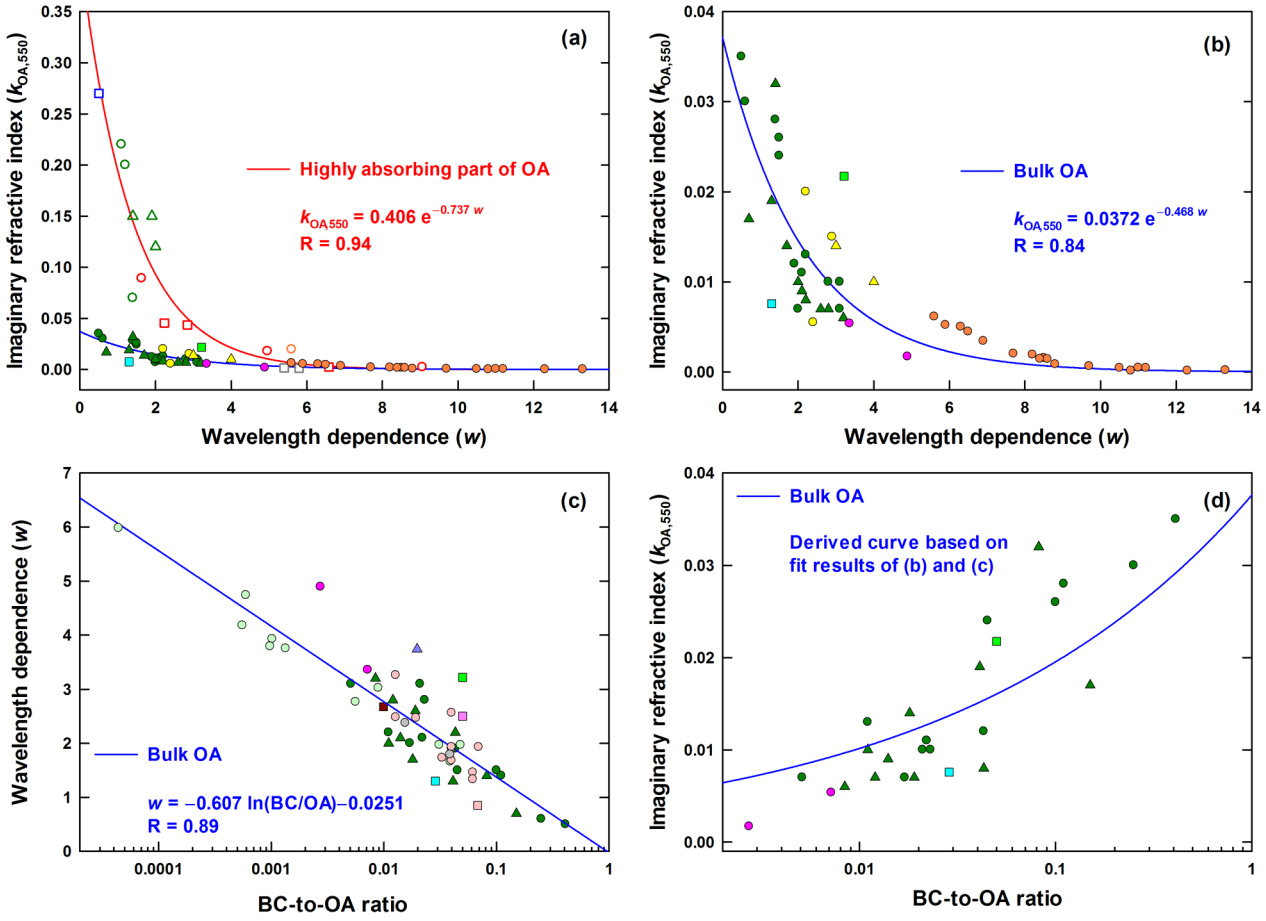

	Bulk OA			OA highly absorbing part			Fuel type / emission sources
	Lab-fresh	Lab-aged	Field	Lab-fresh	Lab-aged	Field	
Saleh et al., 2014	●	▲		○	△		2 boreal forest species, 2 grasses, 2 agricultural wastes
Saleh et al., 2013	●	▲					Oak, pocosin pine, gallberry
Chen and Bond, 2010	●			○			Oak, pine
Kirchstetteret et al., 2004			■				Firewood, redwood needle, African savanna fire
Lack et al., 2012			■				Four-Mile Canyon forest fire
Chakrabarty et al., 2010	●						Duff species
Alexander et al., 2008						□	Biomass plume of East Asian-Pacific outflow
Hoffer et al., 2006						□	Amazon biomass burning
Dinar et al., 2008				○		□	Wood, Suwannee River Fulvic Acid reference sample
Zhong and Jang, 2014		▲					Wood
Sandradewi et al., 2008			■				Wood (mainly beech)
Chakrabarty et al., 2014			■				Funeral pyres
Favez et al., 2009			■				Rice straw
Lewis et al., 2008	●						14 fuel types including pine, flowering shrub, duff, fern, etc.
McMeeking et al., 2014	●						7 typical fuels in prescribed fires and wildfires in the US
Liu et al., 2014	●						20 types of woods and grasses

Figure 1. (a, b) Imaginary refractive index of OA at 550 nm ($k_{OA,550}$) as a function of its wavelength dependence (w) for biomass burning and biofuel combustion sources, and (c) w and (d) $k_{OA,550}$ as a function of the BC-to-OA ratio. (b) Duplication of part a but with a $k_{OA,550}$ scale in the range 0–0.04 and without the open symbols. Different studies are distinguished by color, and their fuel or emission types are summarized in the legend table. Circles, triangles, and squares correspond to fresh emissions measured in the laboratory, chemically aged emissions measured in the laboratory, and field measurements near emission sources, respectively. Blue and red lines in parts a–c are least-squares fits to all filled and open symbols, which represent the measurements for the bulk OA and highly absorbing part of OA, respectively. Blue line in part d is derived from the best fit results of bulk OA in parts b and c using eqs 9 and 10.

absorption and scattering cross sections (MAC and MSC, respectively) of spherical particles (the two most important optical properties) can be derived from m and the particles' size distribution through Mie theory.[30] In current climate and chemical transport models, light absorption properties of POA are poorly represented. Most models still treat POA as nonabsorbing (i.e., k values of OA, k_{OA} = 0) and underestimate the total warming effect of carbonaceous aerosols. For the limited studies that took into account the BrC effects, the treatments were also too simplistic to reflect the variety of reported k_{OA} values, which typically span 2 orders of magnitude. For example, Park et al.[24] calculated the light absorption coefficients of BrC over East Asia in the GEOS-Chem model as a product of the simulated BC concentration, a BrC-to-BC ratio of 1, and a fixed MAC of 3.8 m^2 g^{-1}. Feng et al.[26] treated 66% of the total POA from biofuel/biomass

DOI: 10.1021/acs.est.5b00211
Environ. Sci. Technol. 2015, 49, 4868–4877

emissions as BrC, whereas Lin et al.[31] assumed that all POAs from biomass, biofuel, and residential coal burning were BrC. Both studies used spectrally dependent k_{OA} from Kirchstetter et al.[3] and Chen and Bond[7] as high- and low-absorbing scenarios in their models to evaluate the influence of BrC on the global distribution of radiative forcing (RF). Clearly, better parametrization of the light-absorbing properties of POA is urgently needed in models.

Because BrC is a complex mixture encompassing a large group of organic compounds with various absorptivities and lacking a formal analytical definition,[1,2] we focus on the light-absorbing properties of the bulk POA rather than treat the BrC separately as a POA subset. We first review the currently available k_{OA}-related measurements and develop fuel-type-based k_{OA} spectral profiles, as well as their uncertainties, for POA emitted from both biofuel/biomass and fossil fuel combustion sources. Then, these wavelength-dependent k_{OA} profiles are incorporated into a global POA emission inventory, and the integrated light absorption properties of sectoral and total POA emissions are estimated. We also showed how the POA radiative effect changes when accounting for the POA absorption.

METHODS AND DATA

Data Sets of Biomass/Biofuel Combustion Sources. Currently, the majority of light-absorbing POA studies have focused on the biomass/biofuel combustion sources, because POA emissions from these sources are highly absorptive[2] and contribute ~90% of the global POA budget.[1,32] However, reported k_{OA} values varied substantially among different studies due to the complex and poorly understood chemical nature of the light-absorbing compounds comprising POA. Recently, Saleh et al.[14] found that k_{OA} of biomass burning emissions can be parametrized as a function of the BC-to-OA ratio. Following the same idea, we reviewed the available measurements of absorbing OA from not only biomass burning but also biofuel combustion sources and examined whether the absorption properties of OA from these sources can be linked to the BC-to-OA ratio.

Data sets of biomass/biofuel combustion considered in this work[3−18] are shown in Figure 1. We used laboratory OA measurements of fresh and chemically aged emissions and field OA measurements near intensive biomass/biofuel emission sources. Ambient and remote sensing measurements were discarded because they may be influenced by emissions from a variety of sources and by the presence of secondary organic aerosols (SOAs). We also included a series of well-controlled FLAME (Fire Lab at Missoula Experiment) measurements of biomass smoke.[12,13,17] Because the reported optical properties of these measurements were for the bulk carbonaceous aerosols, only experiments with the OA fraction >95% of the total aerosol mass were included. These data were utilized in Figure 1c only to show the wavelength dependence of the light-absorbing OA in a wide range of BC-to-OA ratios.

We assumed that the k_{OA} has a power-law wavelength dependence[14,33,34] and can be expressed as

$$k_{OA,\lambda} = k_{OA,550} \times (550/\lambda)^{w} \quad (1)$$

where $k_{OA,550}$ is k_{OA} at the wavelength (λ) of 550 nm and w is the wavelength dependence of k_{OA}. For those studies that measure the OA absorption coefficients/efficiencies, w is often described using the absorption Ångström exponent (AAE), where AAE = w + 1 for small particles.[14] We made the following corrections/calculations to reported results not giving $k_{OA,550}$ and/or w directly: (1) For studies reporting the k_{OA} (or absorption coefficients/efficiencies) at multiple wavelengths, w (or AAE) was determined from the linear regression fit of log(k_{OA}) [or log(absorption coefficients/efficiencies)] versus log(λ). (2) Reported or calculated AAE values were converted to w by subtracting 1. (3) For k_{OA} values reported at wavelengths other than 550 nm, $k_{OA,550}$ values were calculated with eq 1. (4) For studies measuring the density-normalized absorption coefficient ($\sigma_{liquid} = \alpha/\rho$) from organic liquid (e.g., methanol and acetone) extracts of POA, k_{OA} was calculated by[34]

$$k_{OA,\lambda} = \rho\sigma_{liquid,\lambda}\lambda/4\pi \quad (2)$$

where ρ is the density of the dissolved compounds and was fixed to 1.2 g cm^{-3}.[35] Note that σ_{liquid} is different from the particulate MAC although they have the same units of m^2 g^{-1}.[34] (5) $k_{OA,550}$ and w of the results of Kirchstetter et al.[3] were corrected to 0.022 and 3.3, respectively (S1 in the Supporting Information). (6) For conversion of the mass of OC (organic carbon) to OA, an OA-to-OC ratio of 2.0 was used, as suggested by Turpin and Lim[35] for biofuel/biomass burning sources.

Monte Carlo Simulations of Ångström Attribution of POA Absorption for Lignite Combustion Sources. Although most of the reported k_{OA} values were focused on biomass/biofuel burning sources, some studies did show that POA emissions from coal,[19,20,23,36,37] oil,[14,21] and propane[22] combustion contain light-absorbing components. We focus on coal in this section and show the treatments of others in the next section.

Bond et al. measured the light-absorbing properties of carbonaceous aerosols emitted from a small industrial boiler burning lignite[19,37] and residential stoves burning both bituminous coal and lignite.[20] They found that light absorption by particles from these low-temperature coal combustion sources exhibited a strong spectral dependence with AAE up to 2.9. They hypothesized that a spectrally dependent k of co-emitted OA is the most plausible explanation of this phenomenon.[36] Unfortunately, they did not provide absorption properties of OA, but only of the bulk carbonaceous aerosols; to our knowledge, there is currently no study reporting the k_{OA} directly for coal combustion sources. Here, we applied the widely used absorption attribution method[3,11,27,38] to the measurements of Bond et al. for the lignite-burning industrial boiler,[19] in order to separate the light absorption by OA from the total aerosol absorption, and retrieved the k_{OA} values through the Mie calculation. This particular data set was chosen because the emissions were well-characterized, and most of the relevant information can be found in a series of subsequent publications.[37,39−41]

The experiments of Bond et al. were conducted at a lignite-burning plant in Leipzig, Germany. MACs for the bulk submicrometer particles were given at four wavelengths (450, 550, 750, and 1000 nm). We assumed that BC and POA were the only light absorbers in the emitted particles. Therefore, the measured MAC at λ can be expressed as

$$\mathrm{MAC}_{\lambda} = f_{BC}\mathrm{MAC}_{BC,\lambda} + f_{POA}\mathrm{MAC}_{POA,\lambda} \quad (3)$$

where f_{BC} and f_{POA} are the mass fractions of BC and POA in the total submicrometer particles, respectively. The light

DOI: 10.1021/acs.est.5b00211
Environ. Sci. Technol. 2015, 49, 4868−4877

absorption was assumed to be attributed solely to ("encapsulated") BC at 1000 nm

$$\mathrm{MAC}_{1000} = f_{\mathrm{BC}}\mathrm{MAC}_{\mathrm{BC},1000} \quad (4)$$

Assuming that the spectral absorption of ("encapsulated") BC follows the power law relationship ($\lambda^{-\mathrm{AAE}_{\mathrm{BC}}}$),[38,42] $\mathrm{MAC}_{\mathrm{BC}}$ at a shorter wavelength is given by

$$\frac{\mathrm{MAC}_{\mathrm{BC},\lambda}}{\mathrm{MAC}_{\mathrm{BC},1000}} = \left(\frac{\lambda}{1000}\right)^{-\mathrm{AAE}_{\mathrm{BC}}} \quad (5)$$

When eqs 3−5 are combined, $\mathrm{MAC}_{\mathrm{POA}}$ at λ was determined as

$$\mathrm{MAC}_{\mathrm{POA},\lambda} = \frac{1}{f_{\mathrm{POA}}}\left[\mathrm{MAC}_{\lambda} - \left(\frac{\lambda}{1000}\right)^{-\mathrm{AAE}_{\mathrm{BC}}}\mathrm{MAC}_{1000}\right] \quad (6)$$

We then performed Mie calculations and optimized the $k_{\mathrm{OA},\lambda}$ until the Mie-predicted $\mathrm{MAC}_{\mathrm{POA},\lambda}$ matched the one estimated by eq 6. Finally, w was determined from the linear regression fit of $\log(k_{\mathrm{OA},\lambda})$ versus $\log(\lambda)$, and k_{OA} over the whole spectrum was derived from eq 1.

We used a Monte Carlo approach to simulate the above processes and determine the uncertainties. The Monte Carlo method is a problem-solving technique that approximates the probability of certain outcomes by running multiple simulations with random variables. In this work, we assigned appropriate probability distributions to all input parameters and performed 10 000 simulations. Unless specified otherwise, the term "uncertainty" in this Article refers to one standard deviation ($\pm 1\sigma$) or the coefficient of variation (CV, σ divided by the mean) expressed as a percentage. We applied normal distributions for MAC measurements with uncertainties of 30% provided by Bond et al.[19] As a key input to the Mie model, POA size distribution was assumed to be similar to the bulk emission with a count mean diameter (CMD) of 50 ± 5 nm and a geometric standard deviation (GSD) of 1.45 ± 0.05.[39−41] We ignored both the ultrafine (CMD ∼4 nm) and the accumulation mode (CMD ∼350 nm) detected in the experiments, since particles in these two modes together accounted for <0.5% of the total particle number.[40] The real refractive index and density of POA in the Mie calculation were assumed to be normally distributed at 1.55 ± 0.15 and 1.2 ± 0.1 g cm^{-3} on the basis of a literature review.[5,8,10,11,14,35,39] The parameter f_{POA} was not quantified by Bond et al., and we assigned it a uniform distribution in the range 0.4−0.9 considering an OA-to-OC ratio of 1.4, suggested for the fossil-fuel-based POA.[35] The lower bound was estimated for lignite-fired boilers in the United States,[43] while the upper bound was from source measurements of home-heating furnaces burning similar lignite in the neighboring Czech Republic.[32,44] Generally, the light absorption of BC is considered to be weakly dependent on wavelength with an $\mathrm{AAE}_{\mathrm{BC}}$ of approximately 1.[1,45] However, an organic coating around an inner BC core could make the $\mathrm{AAE}_{\mathrm{BC}}$ larger or smaller.[27,33] Lack and Langridge[38] reviewed a range of field measurements of "encapsulated" BC and suggested an $\mathrm{AAE}_{\mathrm{BC}}$ of 1.1 ± 0.3. In this study, we adopted this estimate and gave it a normal distribution.

Data Sets of Propane, Diesel, and Gasoline Emission Sources. The same methodology was applied to experimental data measured by Schnaiter et al.,[22] who observed a strong spectral dependence of light absorption by particles formed in a propane diffusion flame. Since propane is the dominant component in liquefied petroleum gas (LPG), the estimated k_{OA} is valuable for this particular source. Among the six experimental results presented by Schnaiter et al., we chose only the experiment with carbon-to-oxygen atomic ratio (C/O) of 0.45 in our analysis. The reasons follow: First, for lower C/O experiments, the AAE values of bulk emissions were close to 1, and the uncertainties in attributed POA absorptions at short wavelengths would be larger than ±100%.[38] Second, for higher C/O experiments, the large measurement errors would not yield statistically significant attributed absorptions. Third, for the chosen C/O = 0.45 experiment, the BC-to-OC ratio was ∼1.5, close to the LPG BC-to-OC emission factor ratio of 1.3 used in emission inventories.[32] For Monte Carlo simulations, 1000 nm in eq 6 was replaced by 700 nm, which was the longest wavelength of measured MAC. From information provided by Schnaiter et al.,[22] the uncertainties of MAC measurements were ±0.5 $\mathrm{m}^2\ \mathrm{g}^{-1}$; CMD, GSD, and f_{POA} were assumed to be normally distributed at 215 ± 22 nm, 1.58 ± 0.05, and 0.6 ± 0.065, respectively.

To the best of our knowledge, only the studies of Saleh et al.[14] and Liu et al.[21] quantify the spectral-dependence of k_{OA} for oil combustion sources. Saleh et al.[14] reported the $k_{\mathrm{OA},550}$ and w for the POA from a 4-cycle 6.6-HP diesel generator. Their results for the fresh POA emissions were used directly in this study. Liu et al.[21] measured the absorption of methanol extracts of freshly emitted POA sampled within 2 m of a major roadway in central Atlanta during a period not significantly impacted by biomass-burning emissions. Since this road-side site had restricted heavy-duty diesel truck access (<5% trucks in terms of traffic volume), we considered their results as the light-absorbing properties of POA from gasoline combustion sources.

Radiative Effect Calculation. We use the concept "simple forcing efficiency" (SFE, W g^{-1}) introduced by Bond and Bergstrom[42] to estimate the first-order clear-sky direct radiative effect of light-absorbing POA emissions. SFE is modified from the direct aerosol RF of Chylek and Wong[46] by normalizing the aerosol mass. Therefore, it represents the energy added to the Earth atmosphere system by a given mass of particles in the atmosphere. A wavelength-dependent version is given as[7]

$$\begin{aligned}\mathrm{SFE} &= \int_{\lambda}\frac{\mathrm{dSFE}}{\mathrm{d}\lambda}\\ &= \int_{\lambda}\left\{-D\frac{\mathrm{d}S(\lambda)}{\mathrm{d}\lambda}{\tau_{\mathrm{atm}}}^{2}(\lambda)(1-F_{\mathrm{c}})[(1-a_{\mathrm{s}})^{2}\beta(\lambda)\right.\\ &\qquad \left.\times \mathrm{MSC}(\lambda) - 2a_{\mathrm{s}}\times \mathrm{MAC}(\lambda)]\right\}\end{aligned} \quad (7)$$

where D is the fractional day length, S is the solar irradiance, τ_{atm} is the atmospheric transmission, F_{c} is the fractional cloud amount, a_{s} is the surface reflectance, and β is the fraction of radiation scattered by aerosol into the upper hemisphere. For the global average calculations, constants used are $D = 0.5$, $F_{\mathrm{c}} = 0.6$, and $a_{\mathrm{s}} = 0.19$, and wavelength-dependent S and τ_{atm} are based on the ASTM G173-03 reference spectra.[7,42] The upscattered fraction β is estimated with a quadratic polynomial, $\beta = 0.0817 + 1.8495b - 2.9682b^2$, where b is the hemispheric backscatter fraction calculated from the ratio of mass cross sections of backscattering to total scattering ($\mathrm{MSC}_{\mathrm{back}}/\mathrm{MSC}$).[47]

DOI: 10.1021/acs.est.5b00211
Environ. Sci. Technol. 2015, 49, 4868−4877

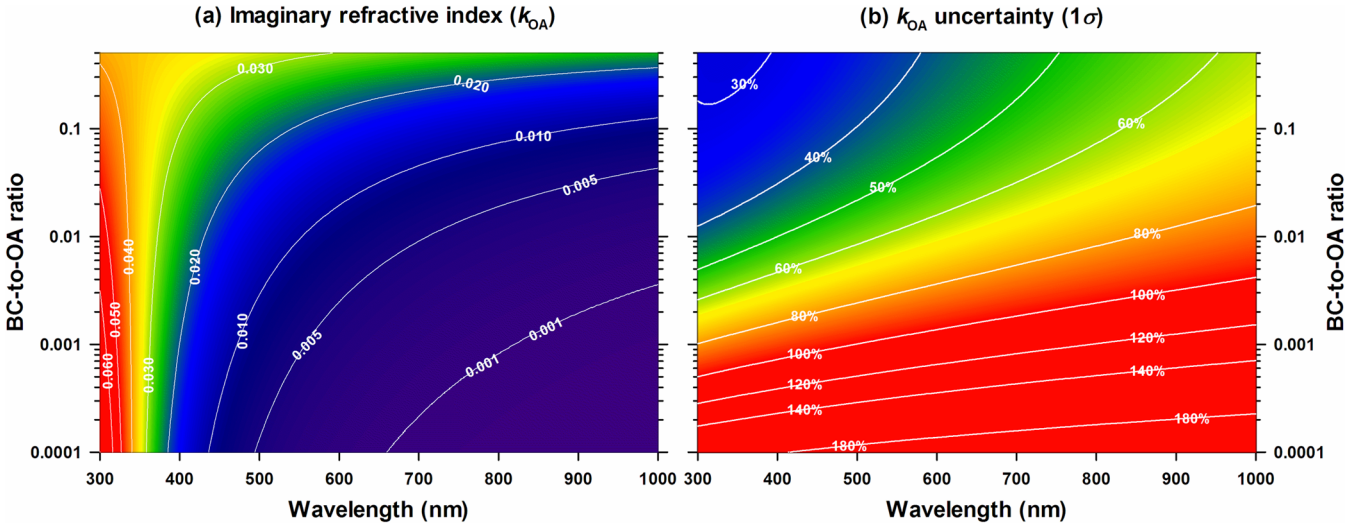

Figure 2. Estimated (a) imaginary refractive index of OA (k_{OA}) and (b) its propagated uncertainty (1σ) as a function of wavelength and BC-to-OA ratio for biomass burning and biofuel combustion sources.

In this study, MSC, MAC, and MSC_{back} were simulated by Mie theory every 1 nm from 300 to 1000 nm. Wavelength-dependent k_{OA} values parametrized in this work were used, and the real refractive index was held constant at 1.55. For simplification, we assumed all POA emissions have log-normal size distributions with a CMD of 160 nm and a GSD of 1.5, which are typically used in models.[31,48] With the Mie simulation results, SFE of POA emissions can be calculated using eq 7 (e.g., curves shown in the abstract figure). Given the global mean column burden of POA (c_{POA}, g m^{-2}), the globally averaged top-of-the-atmosphere clear-sky direct radiative effect (ΔE_R, W m^{-2}, representing the effect of today's aerosol on radiation) can be further calculated as

$$\Delta E_R = \mathrm{SFE} \times c_{POA} \quad (8)$$

RESULTS AND DISCUSSION

k_{OA} of Biomass/Biofuel Combustion Sources. Figure 1 shows the relationships among the $k_{OA,550}$, the wavelength dependence, and the BC-to-OA ratio for OA generated from various biomass/biofuel combustion sources. This depiction can help us understand, to some extent, why the published OA absorption properties vary substantially. Similar to the findings of Saleh et al.,[14] $k_{OA,550}$ of the bulk OA increases (Figure 1d), whereas w of the bulk OA decreases with the BC-to-OA ratio (Figure 1c), despite the differences in biomass/biofuel types, laboratory/field experiments, or fresh/aged aerosols. This implies that the absorptive properties of OA from biomass/biofuel burning depend strongly on burning conditions and weakly on fuel types and atmospheric processing. As an extreme example, Chen and Bond[7] measured the absorption of POA emitted from wood pyrolysis. Since there was nearly no BC formation during the flameless process, the BC-to-OA ratios of their experiments were extremely low, and this might explain why they obtained very high w (>5.5) and very low $k_{OA,550}$ (<0.006).

We found that $k_{OA,550}$ has an inverse relationship with the wavelength dependence w (Figure 1a,b), although the $k_{OA,550}$ values obtained from the bulk OA (filled symbols) are about an order of magnitude smaller than those obtained from the highly absorbing part of OA (open symbols). In the experiments of Saleh et al.,[14] the highly absorbing part of OA refers to the "extremely low-volatility organic compounds" (ELVOC) left after thermally denuding the bulk OA. These compounds account for 8−15% of the total OA mass but are associated with almost all the OA absorption.[14] In the study of Alexander et al.,[8] the optical properties of carbon spheres (i.e., tar balls) were quantified in a vacuum environment where organics with relatively high volatility had been evaporated. Therefore, the studied OA consisted of low-volatility compounds with high absorptivity.[14] Humic-like substances (HULIS) were treated as highly absorbing compounds in the bulk OA, because they have relatively high molecular weight and thus low volatility.[5,10] The highly absorbing component of the OA category also contains one measurement by Chen and Bond,[7] who found that the strongly light-absorbing components of POA from wood pyrolysis were neither water- nor hexane-soluble, but were methanol-soluble. These components accounted for ∼7% of the total OA mass but contributed ∼40% of the total absorbance, and were suggested to be large molecular weight polycyclic aromatic hydrocarbons (PAHs) and oxygenated species.[7]

We next parametrize the k_{OA} of biomass/biofuel burning and its uncertainty as a function of the BC-to-OA ratio. We only included the bulk OA data sets since our purpose is to develop light-absorbing properties for the entire POA emissions. Compared to parts b and c of Figure 1, Figure 1d contains the fewest data points. Therefore, we parametrized the relationships of $k_{OA,550}$ versus w (Figure 1b) and w versus BC-to-OA ratio (Figure 1c) first, and derived the relationship between $k_{OA,550}$ and BC-to-OA ratio subsequently. An exponential and a linear function were used to fit $k_{OA,550}$ versus w and w versus ln(BC-to-OA ratio), respectively, and the fit results are

$$k_{OA,550} = 0.0372e^{-0.468w} \quad (9)$$

$$w = -0.607 \ln(\text{BC-to-OA ratio}) - 0.0251 \quad (10)$$

Via uncertainty propagation, the CV for w and $k_{OA,550}$ as a function of the BC-to-OA ratio can be estimated as

$$CV_w \approx SEE_w/w \quad (11)$$

DOI: 10.1021/acs.est.5b00211
Environ. Sci. Technol. 2015, 49, 4868−4877

$$CV_{k_{OA,550}} \approx \sqrt{(-0.468SEE_w)^2 + (SEE_{k_{OA,550}}/k_{OA,550})^2} \quad (12)$$

where SEE represents the standard error of the estimate of the fit, which is 0.50 and 0.0052 for w and $k_{OA,550}$, respectively. For a given BC-to-OA ratio, $k_{OA,550}$ and w can be calculated using eqs 9 and 10, and k_{OA} over the whole spectrum can be further determined through eq 1. Correspondingly, the uncertainty of k_{OA} can be estimated via the error propagation as

$$CV_{k_{OA}} \approx \{[\ln(550/\lambda)SEE_w]^2 + (CV_{k_{OA,550}})^2 + 2r\ln(550/\lambda)SEE_w CV_{k_{OA,550}}\}^{1/2} \quad (13)$$

The third term in the square root of eq 13 was taken into account because $k_{OA,550}$ and w are not independent variables, as shown in Figure 1b. A Spearman's rank correlation coefficient (r) of −0.864 was calculated on the basis of the used data sets. We also took an absorption measurement uncertainty of 25%[1,38] into account so that the final k_{OA} uncertainty is the sum of the uncertainties in quadrature:

$$CV_{k_{OA}}^{final} \approx \sqrt{(CV_{k_{OA}})^2 + (25\%)^2} \quad (14)$$

Figure 2 shows how k_{OA} of biomass/biofuel sources and its uncertainty vary with wavelength and BC-to-OA ratio. Stronger wavelength-dependent k_{OA} values are observed for lower BC-to-OA ratio conditions (e.g., smoldering combustion), while greater k_{OA} values are observed for higher BC-to-OA ratio conditions (e.g., flaming combustion) at wavelengths >350 nm. The estimated k_{OA} uncertainty increases with wavelength, mainly due to the inverse correlation between $k_{OA,550}$ and w (eq 13). The typical BC-to-OA ratios of the biofuel/biomass combustion sectors in the bottom-up emission inventories are in the range 0.03−0.15,[1,32,49] corresponding to k_{OA} uncertainties in the range 30−70%. We suggest caution in using k_{OA} values estimated under BC-to-OA ratios less than 0.001 since their uncertainties exceed ±100%.

k_{OA} of Fossil Fuel Combustion Sources. Table 1 summarizes the light-absorbing properties of POA generated from the combustion of fossil fuels. For lignite combustion, using the Monte Carlo approach to attribute the POA absorption, we estimated that the $k_{OA,550}$ and w were 0.015 and 2.75, respectively. The w of 2.75 was close to the result of Yang et al.[23] which showed that the average AAE of OA in plumes dominated by residential coal burning emissions near Xianghe, China, was 3.5 (i.e., $w \approx 2.5$). Figure 3 shows the estimated mean k_{OA} for lignite combustion and its uncertainties as a function of wavelength, and the embedded subgraphs display the k_{OA} probability distributions, based on Monte Carlo simulations. The k_{OA} distributions were asymmetric with 95% confidence interval (CI) at 450 nm of −69% to +109%, reflecting the asymmetric response of the Mie calculation to the symmetric inputs. However, we found that the 68.27% CIs (corresponding to ±1σ if normally distributed) were approximately symmetric around the central estimates (e.g., ±43% at 450 nm). Similar results were also found for w distributions with 95% CI of −18% to +30% and 68.27% CI of ±10%. For simplicity, we treated the 68.27% CI as the ±1σ in the following analysis.

Regarding POA from propane combustion, $k_{OA,550}$ and w simulated by the Monte Carlo approach were 0.027 ± 0.014 and 4.62 ± 0.46, respectively (Table 1, Figure S1 in the Supporting Information). Compared to other types of POA, POA generated by propane combustion is much more absorbing over the whole spectrum, and this may be related to its high content of PAH compounds. Slowik et al.[50] analyzed the chemical composition of soot particles generated in a propane/O_2 flame at different combustion conditions using the Aerodyne aerosol mass spectrometer. According to their results, PAH species accounted for >50% of the total OC at the propane-to-air ratio close to the condition studied here. Since PAH species have been suggested[7,51] and proven[52−55] to be strong light absorbers in the UV wavelength range, it is reasonable to conclude that the high content of PAHs in POA led to high light absorption at short wavelengths. PAHs (and other light-absorbing compounds) have also been detected in the particle phase of emissions from oil combustion.[40,56,57] Although they are not the major components of POA, their presence can make the bulk POA absorptive. On the basis of the measurements by Saleh et al.[14] and Liu et al.,[21] estimated

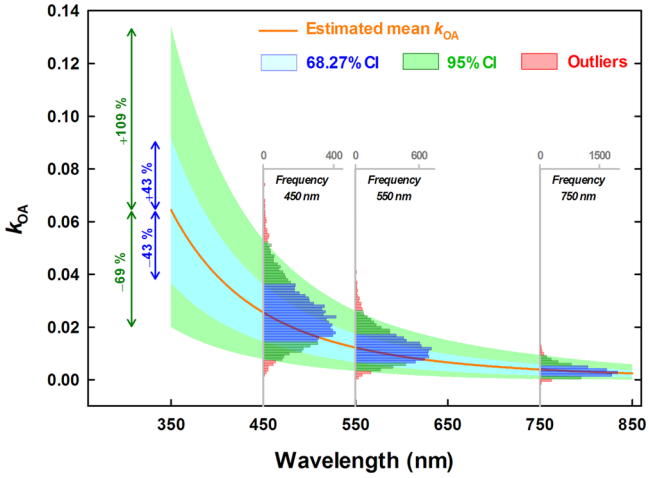

Figure 3. Estimated imaginary refractive index of OA (k_{OA}) as a function of wavelength for the POA emitted from lignite combustion. Subgraphs present the probability distributions of estimated k_{OA} at specified wavelengths. Blue, green, and red shades indicate the 68.27% confidence interval (corresponding to ±1σ), the 95% confidence interval, and the outliers.

Table 1. Summary of Imaginary Refractive Index of POA at 550 nm ($k_{OA,550}$) and Its Wavelength Dependence (w) by Fuel Type[a]

fuel type	$k_{OA,550}$	w	emissions applied to[e]
biomass/biofuel[b]	eq 9, Figure 2	eq 10, Figure 2	biomass/biofuel sources
lignite[b]	1.5×10^{-2} (45%)	2.75 (10%)	brown coal and residential coal sources
diesel[c]	6.0×10^{-3} (40%)	4.40	diesel and heavy fuel oil sources
gasoline[d]	7.4×10^{-4} (45%)	6.16	gasoline sources
propane[b]	2.7×10^{-2} (50%)	4.62 (10%)	LPG sources
other	0	0	all other emission sources

[a]Numbers in parentheses represent one relative standard deviation. [b]Estimated in this study. [c]From Saleh et al.[14] [d]From Liu et al.[21] [e]An additional uncertainty of 50% was assigned to eq 1 derived k_{OA} for fossil fuel sources.

DOI: 10.1021/acs.est.5b00211
Environ. Sci. Technol. 2015, 49, 4868−4877

Table 2. Summary of Light Absorption Properties of POA Emissions and Their Radiative Effect Results

	POA without absorption	POA with absorption parametrized in this work[a]					
		total	RE	IN	PO	TR	BB
$k_{OA,550}$	0	1.7×10^{-2}	2.1×10^{-2}	1.2×10^{-2}	9.1×10^{-3}	3.9×10^{-3}	1.7×10^{-2}
w	0	1.62	1.28	1.55	2.32	4.54	1.70
k_{OA} av uncertainty[b]		51%	49%	51%	62%	64%	52%
POC emission (Tg C year^{-1})	62.3	62.3	11.2	2.0	0.1	1.2	47.8
POA emissions (Tg year^{-1})	123.0	123.0	22.0	3.5	0.1	1.7	95.7
POA load c_{POA} (mg m^{-2})[c]	5.02	5.02	0.90	0.14	0.00	0.07	3.91
SFE average (W g^{-1})[d]	−76.5	−55.5	−51.6	−62.0	−64.6	−69.4	−55.8
ΔE_R (W m^{-2})	−0.384	−0.278	−0.046	−0.009	−0.000	−0.005	−0.218
ΔE_R per emission (μW m^{-2}) (Gg year^{-1})$^{-1}$	−3.12	−2.26	−2.11	−2.53	−2.64	−2.83	−2.28
SFE over snow (W g^{-1})[e]	−4.7	+62.3	+75.5	+41.5	+32.4	+16.6	+61.3

[a]RE, residential; IN, industry; PO, power generation; TR, transportation; BB, open biomass burning. [b]Averaged between 300 and 1000 nm. [c]Assuming a global average POA lifetime of 7.6 days which is the mean of the AeroCom I models.[60] [d]With Earth average surface albedo of 0.19. [e]With surface albedo of 0.8 for snow-covered ground.

$k_{OA,550}$ and w for POA from diesel and gasoline combustion are listed in Table 1.

While only fixed $k_{OA,550}$ and w were given for POA generated from fossil fuel combustion, due to the lack of data, we hypothesize that they both depend on the combustion condition and have relationships with the BC-to-OA ratio similar to the biofuel/biomass case. For example, Bond et al.[20,36] found the MAC of coal-burning aerosols depended on burning conditions, and the AAE of carbonaceous aerosols was larger during the fuel addition phase (low BC-to-OA ratio, AAE = 2.5) than during the active burning phase (high BC-to-OA ratio, AAE = 1.1). In propane combustion, MAC_{550} increased, whereas AAE decreased with the increasing BC-to-OA ratio.[22] The typical BC-to-OA ratio of diesel combustion is higher than that of gasoline,[32] and we indeed obtained larger $k_{OA,550}$ and smaller w values for diesel combustion. More measurements are needed to better quantify the effect of burning conditions on POA light-absorbing properties from fossil fuel combustion sources.

Light Absorption Properties and Radiative Effects of POA Emissions. In this section, we apply the fuel-type-based parametrization of k_{OA} to the global carbonaceous aerosol emissions in the year 2010 and estimate the light absorption properties of POA emissions, as well as their radiative effects. The used BC and OC emission inventories are global extensions of our previous work for China and India.[49] They were built using a technology-based emission model[1,32,49] including five major sectors (i.e., residential, industry, power, transportation, and open biomass burning) and >150 sector/fuel/technology combinations. For the open biomass burning of forests and grasslands, we used emissions from the Quick Fire Emission Dataset (QFED) v2.4.[58,59] Tables S1 and S2 in the Supporting Information list the BC and OC emissions by sector and region. In summary, total global BC and OC emissions were 11.7 and 62.3 Tg C year^{-1}, respectively, in 2010. Using an OA-to-OC ratio of 2.0 for biofuel/biomass-burning sources and a ratio of 1.4 for fossil fuel sources,[35] we estimated global POA emissions of 123 Tg year^{-1}.

For biomass/biofuel combustion sources, we linked the light absorption properties of POA emissions to the parametrized k_{OA} shown in Figure 2 with the BC-to-OA emission ratio. For fossil-fuel-based POA emissions, which contribute only ∼10% of the global budget,[1,32] we simply applied the k_{OA} spectral profiles of lignite, diesel, gasoline, and propane to POA emissions from brown coal, diesel (and fuel oil), gasoline, and LPG combustion sources, respectively (Table 1), and all other POA emission were assumed to be purely scattering. The k_{OA} of lignite combustion was also applied to all residential coal combustion sources, because the inefficient combustion of hard coal in residential stoves/furnaces has been reported to form light-absorbing POA in both laboratory and field measurements.[20,23] Considering that the $k_{OA,550}$ and w values of fossil-fuel-based POA were estimated from limited measurements, and the potential effect of burning conditions was not taken into account, we assigned eq 1 derived k_{OA} an additional uncertainty of 50% based on the authors' judgment. Finally, we calculated the integrated k_{OA} for sector i as

$$k_{OA,i}(\lambda) = \sum_j [k_{OA,i,j}(\lambda) E_{i,j}] / \sum_j E_{i,j} \quad (15)$$

where E represents POA emissions and j is the detailed sector/fuel/technology combinations in sector i.

Table 2 lists the calculated light-absorbing properties of the major sectors, as well as the total POA. The integrated k_{OA} of the global total POA is close to that of the open biomass-burning sector, which dominates (78%) the total POA emissions. Its uncertainty was estimated to be in the range 33−70% depending on the wavelength. Using eq 7, we provide a first-order estimate of the radiative effects of the sectoral and the total POA emissions. As shown in the abstract figure and Table 2, if all POA emissions were nonabsorbing, the global average SFE would be −77 W g^{-1}, which is comparable to values obtained from global climate models (∼80 W g^{-1}).[1,60] ΔE_R per unit POA emission was estimated to be −3.1 (μW m^{-2}) (Gg year^{-1})$^{-1}$, which is also in the range of the best estimate of −4 ± 3 (μW m^{-2}) (Gg year^{-1})$^{-1}$ for purely scattering POA.[1] The negative ΔE_R indicates the cooling effect on the atmosphere.With the inclusion of POA absorptivity, the global average SFE of total emissions increases by 21 W g^{-1} to −56 W g^{-1} (see abstract figure). Although the overall radiative effect is still cooling, the absorption of POA reduces the amount of the negative ΔE_R significantly, demonstrating its warming effect. We estimate a global average absorption radiative effect from POA of +0.11 W m^{-2}, in line with currently available model results of +0.07 to +0.25 W m^{-2}.[25,26,31] The absorptive POA shows even stronger warming effects over bright surfaces such as the Arctic, the Himalayas, and the clouds above. With the calculation repeated for a snow-covered surface with a_s of 0.8, SFE is predicted to be +62 W g^{-1}, in contrast to −5 W g^{-1} with the nonabsorbing POA

DOI: 10.1021/acs.est.5b00211
Environ. Sci. Technol. 2015, 49, 4868−4877

assumption. Full model simulations will be helpful to better quantify the radiative impacts of POA absorption.

Finally, we point out the need for caution when using the light-absorbing properties developed in this work. First, the sectoral (or total) integrated k_{OA} profiles depend on the characteristics of the carbonaceous aerosol emissions. Therefore, they need to be modified according to the specific emissions used. Second, uncertainties presented in this study are associated with the light-absorbing properties only and do not include the influence of emissions, the uncertainties of which are generally about a factor of 2.[1,32,49] Third, the current parametrizations of k_{OA} are based on limited data sets, especially for POA from fossil fuel combustion sources. They should be revisited when more measurement data are available. Furthermore, the effects of mixing and aging as well as SOA formation on the aerosol optical properties will need to be added in models to go beyond our first-order estimates of radiative effect. Nevertheless, this study provides methods and data sets to address the BrC issue at the emission inventory level. When light-absorbing properties are incorporated into emissions, more realistic simulations of POA will be possible and will help us to better understand the climate impacts of POA emissions.

■ ASSOCIATED CONTENT

Supporting Information

Corrections for the results of Kirchstetter et al., Monte Carlo results for the propane combustion, and global BC and OC emissions in 2010. This material is available free of charge via the Internet at http://pubs.acs.org.

■ AUTHOR INFORMATION

Corresponding Author

*E-mail: zlu@anl.gov; phone: (630) 252-9853; fax: (630) 252-8007.

Notes

The information in this document has been subjected to review by the National Center for Environmental Assessment, U.S. EPA, and approved for publication. Approval does not signify that the contents reflect the views of the Agency.

The authors declare no competing financial interest.

■ ACKNOWLEDGMENTS

This work was sponsored by the Office of Biological and Environmental Research in the U.S. Department of Energy (USDOE), Office of Science. We thank Ashley Williamson and Bob Vallario for their support. Argonne National Laboratory is operated by UChicago Argonne, LLC, under Contract No. DE-AC02-06CH11357 with the USDOE. LANL thanks USDOE SC OBER ASR Grant F265 for support.

■ REFERENCES

(1) Bond, T. C.; Doherty, S. J.; Fahey, D. W.; Forster, P. M.; Berntsen, T.; DeAngelo, B. J.; Flanner, M. G.; Ghan, S.; Karcher, B.; Koch, D.; Kinne, S.; Kondo, Y.; Quinn, P. K.; Sarofim, M. C.; Schultz, M. G.; Schulz, M.; Venkataraman, C.; Zhang, H.; Zhang, S.; Bellouin, N.; Guttikunda, S. K.; Hopke, P. K.; Jacobson, M. Z.; Kaiser, J. W.; Klimont, Z.; Lohmann, U.; Schwarz, J. P.; Shindell, D.; Storelvmo, T.; Warren, S. G.; Zender, C. S. Bounding the role of black carbon in the climate system: A scientific assessment. *J. Geophys. Res.* **2013**, *118*, 5380−5552.

(2) Andreae, M. O.; Gelencser, A. Black carbon or brown carbon? The nature of light-absorbing carbonaceous aerosols. *Atmos. Chem. Phys.* **2006**, *6*, 3131−3148.

(3) Kirchstetter, T. W.; Novakov, T.; Hobbs, P. V. Evidence that the spectral dependence of light absorption by aerosols is affected by organic carbon. *J. Geophys. Res.* **2004**, *109*, D21208 DOI: 10.1029/2004jd004999.

(4) Saleh, R.; Hennigan, C. J.; McMeeking, G. R.; Chuang, W. K.; Robinson, E. S.; Coe, H.; Donahue, N. M.; Robinson, A. L. Absorptivity of brown carbon in fresh and photo-chemically aged biomass-burning emissions. *Atmos. Chem. Phys.* **2013**, *13*, 7683−7693.

(5) Dinar, E.; Riziq, A. A.; Spindler, C.; Erlick, C.; Kiss, G.; Rudich, Y. The complex refractive index of atmospheric and model humic-like substances (HULIS) retrieved by a cavity ring down aerosol spectrometer (CRD-AS). *Faraday Discuss.* **2008**, *137*, 279−295.

(6) Chakrabarty, R. K.; Moosmuller, H.; Chen, L. W. A.; Lewis, K.; Arnott, W. P.; Mazzoleni, C.; Dubey, M. K.; Wold, C. E.; Hao, W. M.; Kreidenweis, S. M. Brown carbon in tar balls from smoldering biomass combustion. *Atmos. Chem. Phys.* **2010**, *10*, 6363−6370.

(7) Chen, Y.; Bond, T. C. Light absorption by organic carbon from wood combustion. *Atmos. Chem. Phys.* **2010**, *10*, 1773−1787.

(8) Alexander, D. T. L.; Crozier, P. A.; Anderson, J. R. Brown carbon spheres in East Asian outflow and their optical properties. *Science* **2008**, *321*, 833−836.

(9) Favez, O.; Alfaro, S. C.; Sciare, J.; Cachier, H.; Abdelwahab, M. M. Ambient measurements of light-absorption by agricultural waste burning organic aerosols. *J. Aerosol Sci.* **2009**, *40*, 613−620.

(10) Hoffer, A.; Gelencser, A.; Guyon, P.; Kiss, G.; Schmid, O.; Frank, G. P.; Artaxo, P.; Andreae, M. O. Optical properties of humic-like substances (HULIS) in biomass-burning aerosols. *Atmos. Chem. Phys.* **2006**, *6*, 3563−3570.

(11) Lack, D. A.; Langridge, J. M.; Bahreini, R.; Cappa, C. D.; Middlebrook, A. M.; Schwarz, J. P. Brown carbon and internal mixing in biomass burning particles. *Proc. Natl. Acad. Sci. U.S.A.* **2012**, *109*, 14802−14807.

(12) Lewis, K.; Arnott, W. P.; Moosmuller, H.; Wold, C. E. Strong spectral variation of biomass smoke light absorption and single scattering albedo observed with a novel dual-wavelength photoacoustic instrument. *J. Geophys. Res.* **2008**, *113*, D16203 DOI: 10.1029/2007jd009699.

(13) McMeeking, G. R.; Fortner, E.; Onasch, T. B.; Taylor, J.; Flynn, M.; Coe, H.; Kreidenweis, S. M. Impacts of non-refracory material on light absorption by aerosols emitted from biomass burning. *J. Geophys. Res.* **2014**, *119*, 12272−12286.

(14) Saleh, R.; Robinson, E. S.; Tkacik, D. S.; Ahern, A. T.; Liu, S.; Aiken, A. C.; Sullivan, R. C.; Presto, A. A.; Dubey, M. K.; Yokelson, R. J.; Donahue, N. M.; Robinson, A. L. Brownness of organics in aerosols from biomass burning linked to their black carbon content. *Nat. Geosci.* **2014**, *7*, 647−650.

(15) Sandradewi, J.; Prevot, A. S. H.; Szidat, S.; Perron, N.; Alfarra, M. R.; Lanz, V. A.; Weingartner, E.; Baltensperger, U. Using aerosol light absorption measurements for the quantitative determination of wood burning and traffic emission contributions to particulate matter. *Environ. Sci. Technol.* **2008**, *42*, 3316−3323.

(16) Zhong, M.; Jang, M. Dynamic light absorption of biomass-burning organic carbon photochemically aged under natural sunlight. *Atmos. Chem. Phys.* **2014**, *14*, 1517−1525.

(17) Liu, S.; Aiken, A. C.; Arata, C.; Dubey, M. K.; Stockwell, C. E.; Yokelson, R. J.; Stone, E. A.; Jayarathne, T.; Robinson, A. L.; DeMott, P. J.; Kreidenweis, S. M. Aerosol single scattering albedo dependence on biomass combustion efficiency: Laboratory and field studies. *Geophys. Res. Lett.* **2014**, *41*, 742−748.

(18) Chakrabarty, R. K.; Pervez, S.; Chow, J. C.; Watson, J. G.; Dewangan, S.; Robles, J.; Tian, G. Funeral pyres in South Asia: brown carbon aerosol emissions and climate impacts. *Environ. Sci. Technol. Lett.* **2014**, *1*, 44−48.

(19) Bond, T. C.; Bussemer, M.; Wehner, B.; Keller, S.; Charlson, R. J.; Heintzenberg, J. Light absorption by primary particle emissions

DOI: 10.1021/acs.est.5b00211
Environ. Sci. Technol. 2015, 49, 4868−4877

from a lignite burning plant. *Environ. Sci. Technol.* **1999**, *33*, 3887−3891.
(20) Bond, T. C.; Covert, D. S.; Kramlich, J. C.; Larson, T. V.; Charlson, R. J. Primary particle emissions from residential coal burning: Optical properties and size distributions. *J. Geophys. Res.* **2002**, *107* (D21), 8347 DOI: 10.1029/2001jd000571.
(21) Liu, J.; Bergin, M.; Guo, H.; King, L.; Kotra, N.; Edgerton, E.; Weber, R. J. Size-resolved measurements of brown carbon in water and methanol extracts and estimates of their contribution to ambient fine-particle light absorption. *Atmos. Chem. Phys.* **2013**, *13*, 12389−12404.
(22) Schnaiter, M.; Gimmler, M.; Llamas, I.; Linke, C.; Jager, C.; Mutschke, H. Strong spectral dependence of light absorption by organic carbon particles formed by propane combustion. *Atmos. Chem. Phys.* **2006**, *6*, 2981−2990.
(23) Yang, M.; Howell, S. G.; Zhuang, J.; Huebert, B. J. Attribution of aerosol light absorption to black carbon, brown carbon, and dust in China—interpretations of atmospheric measurements during EAST-AIRE. *Atmos. Chem. Phys.* **2009**, *9*, 2035−2050.
(24) Park, R. J.; Kim, M. J.; Jeong, J. I.; Youn, D.; Kim, S. A contribution of brown carbon aerosol to the aerosol light absorption and its radiative forcing in East Asia. *Atmos. Environ.* **2010**, *44*, 1414−1421.
(25) Wang, X.; Heald, C. L.; Ridley, D. A.; Schwarz, J. P.; Spackman, J. R.; Perring, A. E.; Coe, H.; Liu, D.; Clarke, A. D. Exploiting simultaneous observational constraints on mass and absorption to estimate the global direct radiative forcing of black carbon and brown carbon. *Atmos. Chem. Phys.* **2014**, *14*, 10989−11010.
(26) Feng, Y.; Ramanathan, V.; Kotamarthi, V. R. Brown carbon: A significant atmospheric absorber of solar radiation? *Atmos. Chem. Phys.* **2013**, *13*, 8607−8621.
(27) Kirchstetter, T. W.; Thatcher, T. L. Contribution of organic carbon to wood smoke particulate matter absorption of solar radiation. *Atmos. Chem. Phys.* **2012**, *12*, 6067−6072.
(28) Liu, J. M.; Scheuer, E.; Dibb, J.; Ziemba, L. D.; Thornhill, K. L.; Anderson, B. E.; Wisthaler, A.; Mikoviny, T.; Devi, J. J.; Bergin, M.; Weber, R. J. Brown carbon in the continental troposphere. *Geophys. Res. Lett.* **2014**, *41*, 2191−2195.
(29) Chung, C. E.; Ramanathan, V.; Decremer, D. Observationally constrained estimates of carbonaceous aerosol radiative forcing. *Proc. Natl. Acad. Sci. U.S.A.* **2012**, *109*, 11624−11629.
(30) Bohren, C. F.; Huffman, D. R. *Absorption and Scattering of Light by Small Particles*; John Wiley and Sons: New York, 1983.
(31) Lin, G. X.; Penner, J. E.; Flanner, M. G.; Sillman, S.; Xu, L.; Zhou, C. Radiative forcing of organic aerosol in the atmosphere and on snow: Effects of SOA and brown carbon. *J. Geophys. Res.* **2014**, *119*, 7453−7476.
(32) Bond, T. C.; Streets, D. G.; Yarber, K. F.; Nelson, S. M.; Woo, J. H.; Klimont, Z. A technology-based global inventory of black and organic carbon emissions from combustion. *J. Geophys. Res.* **2004**, *109*, D14203 DOI: 10.1029/2003jd003697.
(33) Lack, D. A.; Cappa, C. D. Impact of brown and clear carbon on light absorption enhancement, single scatter albedo and absorption wavelength dependence of black carbon. *Atmos. Chem. Phys.* **2010**, *10*, 4207−4220.
(34) Sun, H. L.; Biedermann, L.; Bond, T. C. Color of brown carbon: A model for ultraviolet and visible light absorption by organic carbon aerosol. *Geophys. Res. Lett.* **2007**, *34*, L17813 DOI: 10.1029/2007gl029797.
(35) Turpin, B. J.; Lim, H. J. Species contributions to $PM_{2.5}$ mass concentrations: Revisiting common assumptions for estimating organic mass. *Aerosol Sci. Technol.* **2001**, *35*, 602−610.
(36) Bond, T. C. Spectral dependence of visible light absorption by carbonaceous particles emitted from coal combustion. *Geophys. Res. Lett.* **2001**, *28*, 4075−4078.
(37) Bond, T. C.; Charlson, R. J.; Heintzenberg, J. Quantifying the emission of light-absorbing particles: Measurements tailored to climate studies. *Geophys. Res. Lett.* **1998**, *25*, 337−340.
(38) Lack, D. A.; Langridge, J. M. On the attribution of black and brown carbon light absorption using the Angstrom exponent. *Atmos. Chem. Phys.* **2013**, *13*, 10535−10543.
(39) Bond, T. C.; Habib, G.; Bergstrom, R. W. Limitations in the enhancement of visible light absorption due to mixing state. *J. Geophys. Res.* **2006**, *111*, D20211 DOI: 10.1029/2006jd007315.
(40) Bond, T. C.; Wehner, B.; Plewka, A.; Wiedensohler, A.; Heintzenberg, J.; Charlson, R. J. Climate-relevant properties of primary particulate emissions from oil and natural gas combustion. *Atmos. Environ.* **2006**, *40*, 3574−3587.
(41) Wehner, B.; Bond, T. C.; Birmili, W.; Heintzenberg, J.; Wiedensohler, A.; Charlson, R. J. Climate-relevant particulate emission characteristics of a coal fired heating plant. *Environ. Sci. Technol.* **1999**, *33*, 3881−3886.
(42) Bond, T. C.; Bergstrom, R. W. Light absorption by carbonaceous particles: An investigative review. *Aerosol Sci. Technol.* **2006**, *40*, 27−67.
(43) Cai, H.; Wang, M. Q. Consideration of black carbon and primary organic carbon emissions in life-cycle analysis of greenhouse gas emissions of vehicle systems and fuels. *Environ. Sci. Technol.* **2014**, *48*, 12445−12453.
(44) Pinto, J. P.; Stevens, R. K.; Willis, R. D.; Kellogg, R.; Mamane, Y.; Novak, J.; Santroch, J.; Benes, I.; Lenicek, J.; Bures, V. Czech air quality monitoring and receptor modeling study. *Environ. Sci. Technol.* **1998**, *32*, 843−854.
(45) Moosmuller, H.; Chakrabarty, R. K.; Ehlers, K. M.; Arnott, W. P. Absorption Angstrom coefficient, brown carbon, and aerosols: Basic concepts, bulk matter, and spherical particles. *Atmos. Chem. Phys.* **2011**, *11*, 1217−1225.
(46) Chylek, P.; Wong, J. Effect of absorbing aerosols on global radiation budget. *Geophys. Res. Lett.* **1995**, *22*, 929−931.
(47) Delene, D. J.; Ogren, J. A. Variability of aerosol optical properties at four North American surface monitoring sites. *J. Atmos. Sci.* **2002**, *59*, 1135−1150.
(48) Wang, M. H.; Penner, J. E.; Liu, X. H. Coupled IMPACT aerosol and NCAR CAM3 model: Evaluation of predicted aerosol number and size distribution. *J. Geophys. Res.* **2009**, *114*, D06302 DOI: 10.1029/2008jd010459.
(49) Lu, Z.; Zhang, Q.; Streets, D. G. Sulfur dioxide and primary carbonaceous aerosol emissions in China and India, 1996−2010. *Atmos. Chem. Phys.* **2011**, *11*, 9839−9864.
(50) Slowik, J. G.; Stainken, K.; Davidovits, P.; Williams, L. R.; Jayne, J. T.; Kolb, C. E.; Worsnop, D. R.; Rudich, Y.; DeCarlo, P. F.; Jimenez, J. L. Particle morphology and density characterization by combined mobility and aerodynamic diameter measurements. Part 2: Application to combustion-generated soot aerosols as a function of fuel equivalence ratio. *Aerosol Sci. Technol.* **2004**, *38*, 1206−1222.
(51) Jacobson, M. Z. Isolating nitrated and aromatic aerosols and nitrated aromatic gases as sources of ultraviolet light absorption. *J. Geophys. Res.* **1999**, *104*, 3527−3542.
(52) Lee, H. J.; Aiona, P. K.; Laskin, A.; Laskin, J.; Nizkorodov, S. A. Effect of solar radiation on the optical properties and molecular composition of laboratory proxies of atmospheric brown carbon. *Environ. Sci. Technol.* **2014**, *48*, 10217−10226.
(53) Zhang, X. L.; Lin, Y. H.; Surratt, J. D.; Weber, R. J. Sources, composition and absorption Angstrom exponent of light-absorbing organic components in aerosol extracts from the Los Angeles basin. *Environ. Sci. Technol.* **2013**, *47*, 3685−3693.
(54) Desyaterik, Y.; Sun, Y.; Shen, X. H.; Lee, T. Y.; Wang, X. F.; Wang, T.; Collett, J. L. Speciation of "brown" carbon in cloud water impacted by agricultural biomass burning in eastern China. *J. Geophys. Res.* **2013**, *118*, 7389−7399.
(55) Mohr, C.; Lopez-Hilfiker, F. D.; Zotter, P.; Prevot, A. S. H.; Xu, L.; Ng, N. L.; Herndon, S. C.; Williams, L. R.; Franklin, J. P.; Zahniser, M. S.; Worsnop, D. R.; Knighton, W. B.; Aiken, A. C.; Gorkowski, K. J.; Dubey, M. K.; Allan, J. D.; Thornton, J. A. Contribution of nitrated phenols to wood burning brown carbon light absorption in Detling, United Kingdom during winter time. *Environ. Sci. Technol.* **2013**, *47*, 6316−6324.

DOI: 10.1021/acs.est.5b00211
Environ. Sci. Technol. 2015, 49, 4868−4877

(56) Eiguren-Fernandez, A.; Miguel, A. H. Size-resolved polycyclic aromatic hydrocarbon emission factors from on-road gasoline and diesel vehicles: Temperature effect on the nuclei-mode. *Environ. Sci. Technol.* **2012**, *46*, 2607−2615.
(57) Perrone, M. G.; Carbone, C.; Faedo, D.; Ferrero, L.; Maggioni, A.; Sangiorgi, G.; Bolzacchini, E. Exhaust emissions of polycyclic aromatic hydrocarbons, n-alkanes and phenols from vehicles coming within different European classes. *Atmos. Environ.* **2014**, *82*, 391−400.
(58) Petrenko, M.; Kahn, R.; Chin, M.; Soja, A.; Kucsera, T. Harshvardhan The use of satellite-measured aerosol optical depth to constrain biomass burning emissions source strength in the global model GOCART. *J. Geophys. Res.* **2012**, *117*, D18212 DOI: 10.1029/2012jd017870.
(59) Darmenov, A.; da Silva, A. M. *The Quick Fire Emissions Dataset (QFED)—Documentation of Versions 2.1, 2.2 and 2.4*; NASA: Washington, DC, 2013.
(60) Schulz, M.; Textor, C.; Kinne, S.; Balkanski, Y.; Bauer, S.; Berntsen, T.; Berglen, T.; Boucher, O.; Dentener, F.; Guibert, S.; Isaksen, I. S. A.; Iversen, T.; Koch, D.; Kirkevag, A.; Liu, X.; Montanaro, V.; Myhre, G.; Penner, J. E.; Pitari, G.; Reddy, S.; Seland, O.; Stier, P.; Takemura, T. Radiative forcing by aerosols as derived from the AeroCom present-day and pre-industrial simulations. *Atmos. Chem. Phys.* **2006**, *6*, 5225−5246.

DOI: 10.1021/acs.est.5b00211
Environ. Sci. Technol. 2015, 49, 4868−4877